Title

Human resistin protects against endotoxic shock by blocking LPS–TLR4 interaction

Journal

Proceedings of the National Academy of Sciences of the United States of America, 114(48)

ISSN

0027-8424

Authors

Jang, Jessica C
Li, Jiang
Gambini, Luca
et al.

Publication Date

2017-11-28

DOI

10.1073/pnas.1716015114

Peer reviewed

Human resistin protects against endotoxic shock by blocking LPS–TLR4 interaction

Jessica C. Jang[a,1], Jiang Li[a,1], Luca Gambini[a], Hashini M. Batugedara[a], Sandeep Sati[b], Mitchell A. Lazar[c,d], Li Fan[b], Maurizio Pellecchia[a], and Meera G. Nair[a,2]

[a]Division of Biomedical Sciences, University of California, Riverside, CA 92521; [b]Biochemistry Department, University of California, Riverside, CA 92521; [c]Institute for Diabetes, Obesity, and Metabolism, Perelman School of Medicine, University of Pennsylvania, Philadelphia, PA 19104; and [d]Division of Endocrinology, Diabetes, and Metabolism, Perelman School of Medicine, University of Pennsylvania, Philadelphia, PA 19104

Edited by Genhong Cheng, University of California, Los Angeles, CA, and accepted by Editorial Board Member Tadatsugu Taniguchi October 20, 2017 (received for review September 12, 2017)

Helminths trigger multiple immunomodulatory pathways that can protect from sepsis. Human resistin (hRetn) is an immune cell-derived protein that is highly elevated in helminth infection and sepsis. However, the function of hRetn in sepsis, or whether hRetn influences helminth protection against sepsis, is unknown. Employing hRetn-expressing transgenic mice (h*RETN*Tg$^+$) and recombinant hRetn, we identify a therapeutic function for hRetn in lipopolysaccharide (LPS)-induced septic shock. hRetn promoted helminth-induced immunomodulation, with increased survival of *Nippostrongylus brasiliensis* (*Nb*)-infected h*RETN*Tg$^+$ mice after a fatal LPS dose compared with naive mice or *Nb*-infected h*RETN*Tg$^-$ mice. Employing immunoprecipitation assays, h*RETN*Tg$^+$*Tlr4*$^{-/-}$ mice, and human immune cell culture, we demonstrate that hRetn binds the LPS receptor Toll-like receptor 4 (TLR4) through its N terminal and modulates STAT3 and TBK1 signaling, triggering a switch from proinflammatory to anti-inflammatory responses. Further, we generate hRetn N-terminal peptides that are able to block LPS proinflammatory function. Together, our studies identify a critical role for hRetn in blocking LPS function with important clinical significance in helminth-induced immunomodulation and sepsis.

resistin | LPS | sepsis | TLR4 | inflammation

In the United States, 750,000 people are diagnosed with sepsis each year, with a mortality rate of 30% (1). Sepsis pathogenesis is exacerbated by the inflammatory response to the pathogen-associated molecular pattern ligand lipopolysaccharide (LPS), a main component of Gram-negative bacterial cell walls. LPS binds to Toll-like receptor 4 (TLR4) and induces a NF-κB-dependent inflammatory cascade resulting in excessive production of tumor necrosis factor alpha (TNFα) and interleukin 6 (IL-6). These proinflammatory cytokines are initially beneficial in bacterial killing, but eventually damage the host's cells and tissues. For instance, excessive production of TNFα causes endothelial cell injury, leading to vascular permeability, low blood pressure, and organ failure (2). Recent studies have targeted this innate inflammatory pathway as a potential treatment for sepsis. *Tlr4*$^{-/-}$ mice or mice treated with anti-TLR4 antibodies were resistant to *Escherichia coli*-induced sepsis as a result of reduced proinflammatory cytokines (3). Nonetheless, clinical trials with anti-TLR4 antibodies or TLR4 antagonists have not been successful (4), and treatment for sepsis is currently limited to antibiotics and supportive care. Epidemiological studies show that sepsis can result from other infections, including Gram-positive bacteria, viruses, or fungi, which also stimulate an excessive inflammatory response (1). Given the lack of specific treatments for sepsis and the high incidence of sepsis in multiple infections, it is critical to identify regulatory pathways that mitigate sepsis pathogenesis.

Helminth infections trigger multiple immunomodulatory pathways that protect against inflammatory diseases including nflammatory bowel disease and sepsis (5, 6). Helminths can cause debilitating symptoms including anemia, intestinal blockage, and malnutrition, therefore, identifying the specific pathways that are protective against inflammatory diseases is necessary to avoid the pathogenic consequences of helminth infection. Recent studies have shown that chronic infection with filarial nematode *Litomosoides sigmodontis* protects mice from fatal sepsis through TLR2-dependent activation of macrophages and inhibition of proinflammatory cytokines (6). In addition, helminth antigens such as *Acanthocheilonema viteae* ES-62 and *Fasciola hepatica* fatty acid binding protein bind to TLR4 and reduce proinflammatory cytokine production (7, 8).

Human resistin (hRetn), a member of the resistin-like molecule (RELM) family of secreted proteins, is expressed in many inflammatory diseases, such as diabetes (9), atherosclerosis (10), and rheumatoid arthritis (11). A recent study identifying a causal link between the immune system and chronic fatigue syndrome reported differential resistin expression. Intriguingly, they found that resistin levels correlated with reduced disease severity in patients with moderate to severe disease, but observed the opposite trend in mild to moderate disease groups (12). Elevated hRetn expression is also observed in infectious settings, including helminth, bacterial, and viral infection (13, 14), and in sepsis (15). Several studies have shown that LPS promotes high-level expression of hRetn in vitro and in vivo (16, 17). Functionally, hRetn increased the production of proinflammatory cytokines, promoted the formation of

Significance

Gram-negative bacterial sepsis is a life-threatening disease that is exacerbated by an uncontrolled immune response to the endotoxin lipopolysaccharide (LPS). Human resistin is a highly expressed cytokine in sepsis, where it is hypothesized to exacerbate inflammation. We identify an unexpected protective role for resistin in endotoxic shock. We use human resistin-expressing transgenic mice and human immune cell assays to show that resistin prevents LPS-induced mortality by blocking LPS binding to its receptor Toll-like receptor 4 (TLR4) and by promoting anti-inflammatory signaling. Helminth infection-induced resistin and treatment with recombinant resistin or resistin N-terminal peptides also inhibited LPS function. These studies report a protective function for resistin and identify the therapeutic potential of resistin-mediated anti-inflammatory pathways or resistin-based reagents in sepsis.

Author contributions: J.C.J., J.L., H.M.B., M.P., and M.G.N. designed research; J.C.J., J.L., L.G., H.M.B., L.F., M.P., and M.G.N. performed research; J.C.J., J.L., L.G., S.S., M.A.L., L.F., M.P., and M.G.N. contributed new reagents/analytic tools; J.C.J., J.L., L.G., S.S., and M.G.N. analyzed data; and J.C.J., J.L., and M.G.N. wrote the paper.

The authors declare no conflict of interest.

This article is a PNAS Direct Submission. G.C. is a guest editor invited by the Editorial Board.

[1]J.C.J. and J.L. contributed equally to this work.

[2]To whom correspondence should be addressed. Email: meera.nair@ucr.edu.

This article contains supporting information online at www.pnas.org/lookup/suppl/doi:10.1073/pnas.1716015114/-/DCSupplemental.

neutrophil extracellular traps, and exacerbated acute LPS-induced lung injury (18). In clinical reports, increased circulating hRetn has been correlated with the severity of sepsis, leading to the suggestion of hRetn as a diagnostic marker of sepsis (15). However, mechanistic studies investigating the function of hRetn in sepsis have not been performed.

Here, we use transgenic mice that express hRetn (h*RETN*Tg$^+$) to study the function of hRetn in a mouse model of sepsis. LPS injection resulted in significantly increased circulating hRetn in the h*RETN*Tg$^+$ mice, which were critically protected against fatal LPS-induced inflammation compared with littermate control h*RETN*Tg$^-$ mice. Further, therapeutic treatment with recombinant hRetn protected C57BL/6 mice against LPS-induced mortality. We tested whether hRetn contributed to helminth-induced immunomodulation and observed that hRetn enhanced the protective effects of *Nippostrongylus brasiliensis* (*Nb*) infection in LPS-induced endotoxic shock. Mechanistically, hRetn inhibited LPS-induced neutrophilia and promoted a shift from a proinflammatory signaling (e.g., TNFα, NF-κB) to an anti-inflammatory pathway (e.g., IL-10, STAT3). hRetn has been proposed to bind TLR4 (19); however, more recent studies have questioned this interaction (20). Combining protein modeling, hRetn *N*-peptide synthesis, and immunoprecipitation assays, we provide direct evidence that hRetn binds TLR4 through the N-terminal helix and competes for the binding of the coreceptor MD2. In functional assays with human peripheral blood mononuclear cells (PBMC), we show that hRetn binding to TLR4 prevents subsequent LPS binding and inflammatory function through a STAT3- and TBK1-dependent mechanism. To test the effect of hRetn on TLR4 signaling in vivo, we generated h*RETN*Tg$^+$ mice on the *Tlr4*$^{-/-}$ background and observed that the anti-inflammatory effects of hRetn were TLR4-dependent. Together, our studies identify a previously unrecognized role for hRetn in blocking LPS function and promoting anti-inflammatory pathways with important clinical implications for helminth-induced immunomodulation and sepsis.

Results

hRETNTg$^+$ Mice Are Resistant to LPS-Induced Inflammation and Mortality. Previous studies have shown that LPS induces expression of h*RETN*, which promotes proinflammatory cytokines, and that septic patients exhibit a high level of circulating hRetn (15). These data suggest hRetn is pathogenic in LPS-induced inflammation and sepsis; however, functional studies testing hRetn effects on sepsis pathogenesis have not been performed. To investigate this in vivo, we used transgenic mice that express hRetn (h*RETN*Tg$^+$) in a mouse model of LPS-induced septic shock (Fig. 1*A*). h*RETN*Tg$^+$ mice were previously generated by bacterial artificial chromosome-mediated integration of the h*RETN* gene and regulatory region on a mouse resistin (m*Retn*$^{-/-}$) background. Characterization of these mice revealed that circulating hRetn levels are comparable to humans and that hRetn is significantly upregulated in vivo after LPS injection (16, 17). In our studies, mice were challenged intraperitoneally (i.p.) with a low dose of LPS to induce hRetn expression in h*RETN*Tg$^+$ mice, followed by a second fatal dose of LPS. Low-dose LPS led to significantly increased circulating hRetn in the h*RETN*Tg$^+$ mice (Fig. 1*B*). Strikingly, hRetn expression was protective against the fatal LPS dose, with significantly improved survival of h*RETN*Tg$^+$ mice compared with littermate control h*RETN*Tg$^-$ mice (Fig. 1*C*, blue vs. black). Although this two-dose LPS model may result in some endotoxin tolerance, this tolerance was not sufficient to protect against fatal endotoxic shock in the absence of hRetn. We investigated the physiological and immune mechanism by which hRetn protected against LPS-induced mortality. Compared with h*RETN*Tg$^-$ mice, h*RETN*Tg$^+$ mice were protected from LPS-induced hypothermia (Fig. 1*D*). Flow cytometric analysis of the peritoneal exudate cells (PEC) from naive mice revealed equivalent frequencies of macrophages, neutrophils, and monocytes, but increased eosinophils in h*RETN*Tg$^+$ mice compared with h*RETN*Tg$^-$ mice (Fig. 1*E*). After LPS treatment, the protective response in h*RETN*Tg$^+$ mice coincided with significantly reduced neutrophils and increased eosinophils compared with h*RETN*Tg$^-$ mice, suggesting a shift from a proinflammatory response to a T helper type 2 immune response. We also observed a significant increase in monocyte frequency, consistent with our previous finding that hRetn promotes monocyte recruitment (13). To identify cytokines that may contribute to hRetn-mediated protection against sepsis, we analyzed by Luminex the serum of LPS-treated h*RETN*Tg$^-$ or h*RETN*Tg$^+$ mice for a panel of 33 cytokines (Table S1). LPS-treated h*RETN*Tg$^+$ mice exhibited a decrease in circulating proinflammatory and Th1 cytokines [e.g., TNFα, interferon gamma (IFNγ), IL-6, IL-12, IL-1α, and granulocyte-macrophage colony-stimulating factor (GM-CSF)] compared with h*RETN*Tg$^-$ mice (Fig. 1 *F* and *G*). Conversely, the anti-inflammatory cytokine IL-10 was increased in h*RETN*Tg$^+$ mice.

Given that the h*RETN* transgene was randomly integrated into the mouse genome, the protective effects observed in the transgenic mice could be a result of disruption of another gene. We generated a second transgenic mouse line (Tg2) and confirmed high circulating hRetn levels after LPS treatment (Fig. 1*B*). Compared with h*RETN*Tg$^-$ mice, Tg2 mice were also protected against the fatal LPS dose, exhibiting 100% survival (Fig. 1*C*, green). We also used single nucleotide polymorphism analysis, available at Dartmouse, to locate the h*RETN* gene insertion sites in the transgenic mice at a resolution of 0.5 Mbp. In both transgenic mouse lines, h*RETN* gene insertions were predicted in noncoding regions or intron sites (Table S2). Because the h*RETN* transgene insertion did not disrupt coding regions, and there is no overlap between insert locations in the h*RETN*Tg$^+$ and Tg2 mice, it is unlikely that the protection conferred by the h*RETN* transgene in both mouse lines is an artifact of the transgene insertion. Both h*RETN* transgenic mouse lines were generated on a m*Retn*$^{-/-}$ background; therefore, we included C57BL/6 mice in the LPS-induced septic shock model to account for potential effects of endogenous mRetn. In contrast to h*RETN*Tg$^+$ mice, C57BL/6 mice succumbed to the fatal LPS dose and mortality was correlated with increased circulating inflammatory cytokines (IL-6, TNFα, and IFNγ) and decreased IL-10. Interestingly, C57BL/6 mice had increased serum IL-6 and IFNγ over h*RETN*Tg$^-$ mice, suggesting endogenous mRetn may increase these cytokines. However, this potential functional effect of mRetn did not affect survival outcome, with no significant differences in survival rate between h*RETN*Tg$^-$ and C57BL/6 mice.

Together, these data identify an anti-inflammatory role for hRetn in endotoxic shock. Because neutrophils contribute to sepsis progression through the production of reactive oxygen species and proinflammatory cytokines (21), the reduction of neutrophils and proinflammatory cytokines in hRetn-expressing mice likely contributes to the reduced mortality during endotoxic shock. The increase in IL-10 may be a result of the increase in eosinophil numbers, as eosinophils have been shown to be a significant source of IL-10 (22). Alternatively, monocytes, potentially induced by the increased macrophage colony-stimulating factor (M-CSF) in the h*RETN*Tg$^+$ mice, may have contributed to the increase in IL-10. This report shows a protective function for hRetn in reducing fatal LPS-induced mortality and challenges the current paradigm that resistin is an inflammatory cytokine that exacerbates sepsis pathogenesis.

Therapeutic Administration of hRetn Ameliorates LPS-Induced Inflammation and Mortality. As a complementary approach to h*RETN*Tg$^+$ mice, we investigated whether intraperitoneal (i.p.) treatment with recombinant hRetn was protective against endotoxic shock (Fig. 2*A*). Because we used recombinant hRetn in C57BL/6 mice, a preliminary dose of LPS was not necessary to

induce hRetn expression and limited confounding factors caused by potential endotoxin tolerance. Compared with control C57BL/6 mice, which succumbed to LPS-induced sepsis, mice treated with recombinant hRetn were resistant to LPS-induced mortality (Fig. 2*B*). hRetn-mediated effects were associated with a modest protection from the LPS-induced temperature drop, and significantly reduced LPS-induced vascular permeability (Fig. 2 *C* and *D*). Associated with hRetn-mediated protection from sepsis pathogenesis, we observed a significant reduction in proinflammatory cytokines TNFα, IL-6, and IFNγ, but no change in IL-10 expression (Fig. 2*E*). Similar to the h*RETN*Tg$^+$ mice, hRetn-treated mice exhibited significantly reduced LPS-induced neutrophils in the peritoneal cavity and increased monocytes (Fig. 2*F*). The recombinant hRetn used was generated in bacteria, but had an undetectable endotoxin (≤0.016 U/μg) when quantified by the *limulus* amebocyte lysate (LAL) assay. Together, these results demonstrate that both transgenic expression of h*RETN* and hRetn treatment are critically protective in a mouse model of sepsis by limiting proinflammatory cytokine expression. Treatment with hRetn did not entirely recapitulate the phenotype in h*RETN*Tg$^+$ mice; notably, the differences in eosinophils and IL-10 expression. These differences are possibly a result of effects of timing of expression, or half-life or localization of the recombinant hRetn. Nonetheless, the protective effect of exogenous hRetn treatment supports the therapeutic potential of hRetn in altering the outcome of septic shock.

Helminth Infection-Induced hRetn Protects Against Sepsis. Helminth infections are associated with an increase in circulating LPS, presumably because of organ damage or an increase in intestinal barrier permeability (23). However, there are numerous helminth-mediated immunoregulatory mechanisms in place to limit excessive LPS inflammatory responses, including sepsis (6). We previously showed that both filarial nematode- and soil-transmitted helminth-infected individuals exhibited increased circulating hRetn (13). In addition, *Nb*-infected h*RETN*Tg$^+$ mice had significantly elevated hRetn in the infected tissue, which impaired optimal helminth expulsion. We hypothesized that instead of

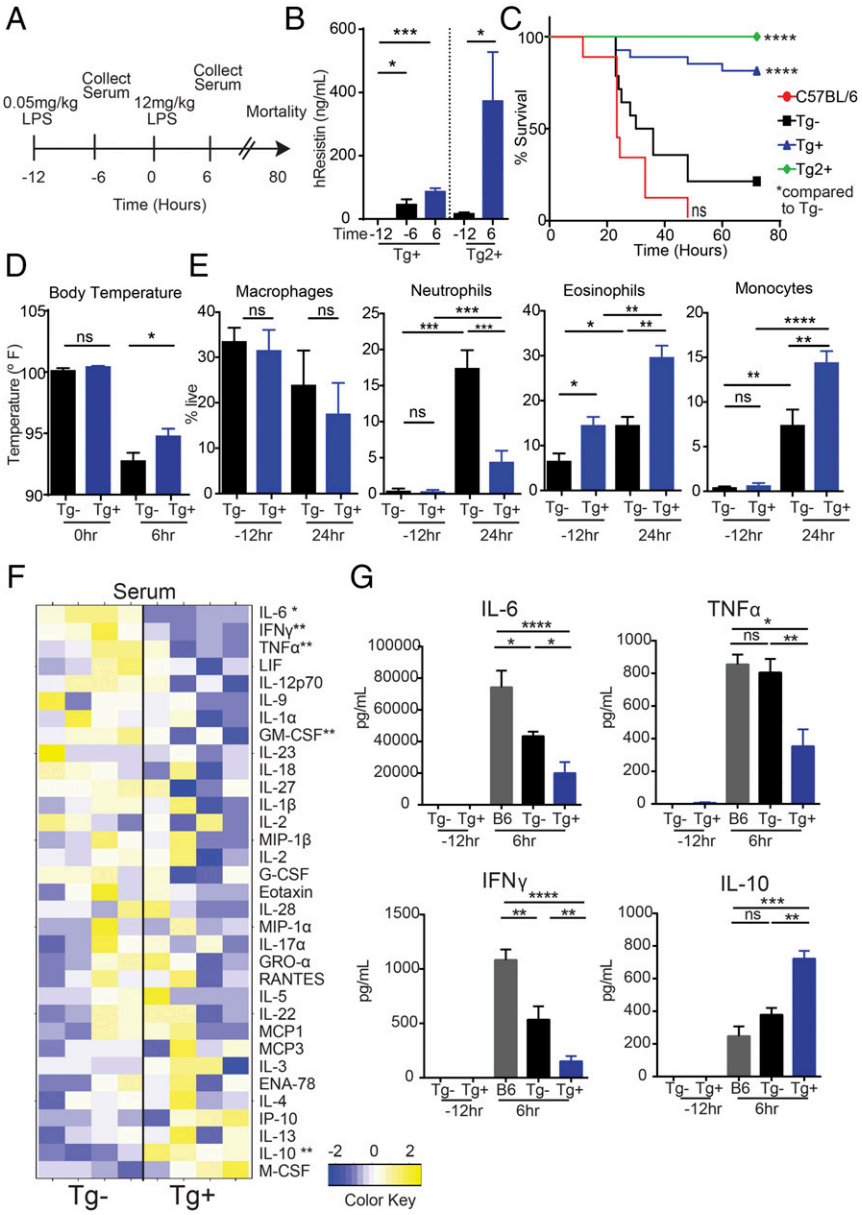

Fig. 1. hRetn protects against endotoxic shock. (*A*) Experimental design of LPS-induced sepsis model. (*B*) hRetn serum levels in h*RETN*Tg$^+$ and Tg2$^+$ mice were measured by ELISA. (*C*) Survival rate was evaluated after high-dose LPS (12 mg/kg) injection. (*D*) Rectal body temperature was measured at 0 and 6 h after high-dose LPS injection. (*E*) h*RETN*Tg$^-$ and h*RETN*Tg$^+$ mice were left naive or challenged with LPS, followed by PEC recovery and flow cytometric analysis at 24 h after high-dose LPS. (*F* and *G*) Serum was assayed for cytokines by Luminex. (*F*) Cytokines induced 6 h after LPS treatment of h*RETN*Tg$^+$ and h*RETN*Tg$^-$ mice were plotted as a heat map. (*G*) Significantly changed proinflammatory and anti-inflammatory cytokines are represented in bar graphs. Data are presented as mean ± SEM (n = 7–12 for survival, n = 3–5 for other parameters) and representative of three separate experiments. ns, not significant; *$P \leq 0.05$; **$P \leq 0.01$; ***$P \leq 0.001$; ****$P \leq 0.0001$.

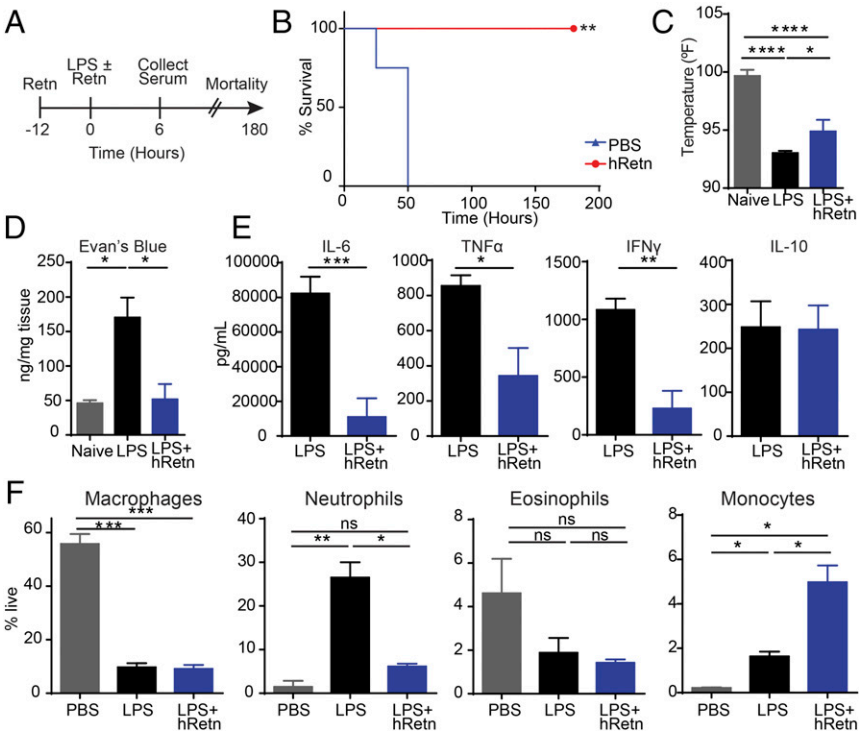

Fig. 2. Therapeutic administration of hRetn during septic shock. (*A*) Experimental design to test the role of hRetn in LPS-induced sepsis. (*B*) Survival rate of C57BL/6 mice treated with PBS or 500 ng/mouse hRetn before LPS injection. (*C*) Rectal body temperature at 6 h after LPS injection. (*D*) Lung vascular permeability was measured with Evan's blue dye at 24 h after LPS injection. (*E*) Serum cytokines at 6 h after LPS injection were measured by Luminex. (*F*) PECs were recovered at 24 h after LPS injection and cells analyzed by flow cytometry. Data are presented as mean ± SEM ($n = 6$ for survival, $n = 3$–5 for other parameters) and are representative of two separate experiments. ns, not significant; $^{*}P \leq 0.05$; $^{**}P \leq 0.01$; $^{***}P \leq 0.001$; $^{****}P \leq 0.0001$.

promoting anti-helminth immunity, hRetn may limit bacterial or LPS-induced inflammatory responses. To investigate this possibility, naive or day 14 *Nb*-infected h*RETN*Tg^{+} and h*RETN*Tg^{-} mice were injected with a fatal dose of LPS and monitored for symptoms of septic shock for 48 h. As opposed to the previous models of endotoxic shock in which hRetn expression or treatment occur 12 h before fatal LPS challenge, this model investigated the effect of *Nb*-induced hRetn over the course of 14 d. Circulating hRetn was modestly increased in *Nb*-infected mice, but significantly increased after LPS challenge compared with naive mice, (Fig. 3*A*). Although all naive h*RETN*Tg^{-} mice succumbed to the fatal LPS dose, naive h*RETN*Tg^{+} mice were more resistant to endotoxic shock with 50% survival, suggesting homeostatic hRetn levels are protective (Fig. 3*B*). *Nb* infection conferred partial protection to h*RETN*Tg^{-} mice; however, this protective effect was significantly enhanced by hRetn (100% survival of *Nb*-infected h*RETN*Tg^{+} mice). Cytokine quantification of the serum from *Nb*-infected mice revealed equivalent levels of LPS-induced monocyte chemoattractant protein 1 (MCP1), IFNγ, IL-6, and IL-10 (Fig. 3*C*). This was in contrast to the low- and high-dose LPS challenge, where there was significantly reduced IFNγ and, conversely, increased IL-10. Given

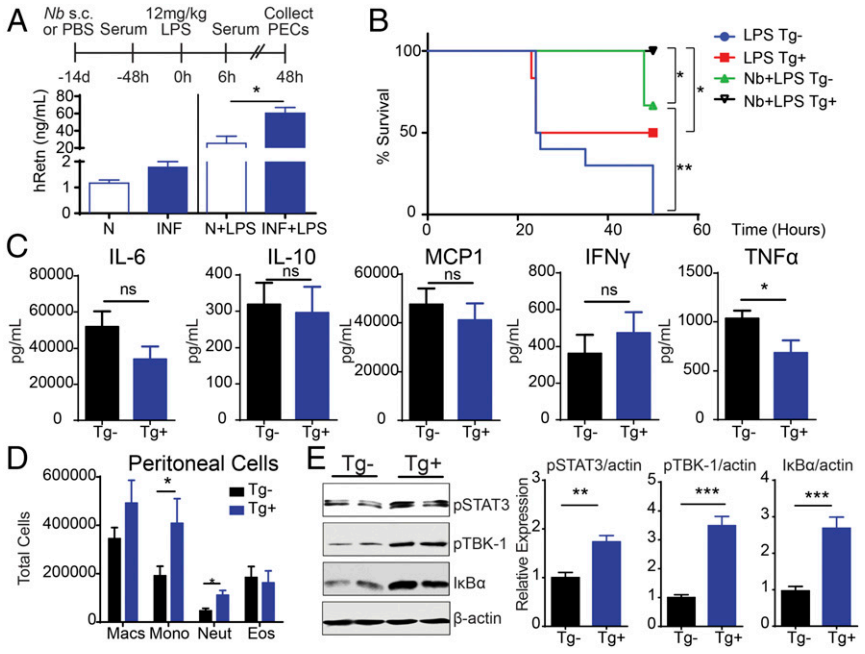

Fig. 3. hRetn enhances helminth-mediated protection during endotoxic shock. (*A*) Experimental design of h*RETN*Tg^{-} and h*RETN*Tg^{+} mice infected with *Nb* for 14 d followed by LPS challenge. Serum hRetn was measured in naive (n) or *Nb*-infected mice at −48 h (*Left*) or 6 h (*Right*) after LPS injection. (*B*) Survival rate after LPS injection. (*C*) Serum cytokines from *Nb*-infected and LPS-challenged h*RETN*Tg^{-} and h*RETN*Tg^{+} mice were evaluated by Luminex. (*D* and *E*) PECs from *Nb*+LPS mice were recovered at 48 h after LPS challenge and assayed directly ex vivo. (*D*) Flow cytometric analysis of PEC populations. (*E*) Representative Western blot (*Left*) and band density of phosphorylated STAT3, phosphorylated TBK1, and IκBα over endogenous β-actin was quantified for three mice per group (*Right*). Data are presented as mean ± SEM ($n = 6$–10 for survival, $n = 3$–4 for other parameters) and are representative of two separate experiments. ns, not significant; $^{*}P \leq 0.05$; $^{**}P \leq 0.01$; $^{***}P \leq 0.001$.

that mice were infected with *Nb* 14 d before LPS challenge, it is possible that *Nb*-induced IL-10 in the h*RETN*Tg$^+$ mice may have occurred earlier, or that in this chronic situation, the effect of hRetn in reducing TNFα is more significant than its effect in increasing IL-10.

Flow cytometric analysis of the peritoneal cavity of *Nb*-infected mice revealed significantly increased neutrophils and monocytes in the h*RETN*Tg$^+$ mice (Fig. 3*D*). These data suggest that although hRetn induced by low-dose LPS and *Nb* infection both protect from septic shock, the underlying immune mechanism of protection may be different. The increased infiltration of neutrophils in *Nb*-infected h*RETN*Tg$^+$ mice suggests that neutrophils are not the direct cause of hRetn-mediated protection in this context and may not be inflammatory in helminth infection. Indeed, previous studies have shown that *Nb*-induced neutrophils exhibit significant differences in function and gene expression compared with LPS-induced neutrophils, including a shift from type 1 to type 2 cytokine responses (24). We next investigated whether *Nb*-induced hRetn influenced pro- and anti-inflammatory signaling after LPS injection. Peritoneal cells from *Nb*+LPS-treated h*RETN*Tg$^-$ and h*RETN*Tg$^+$ mice were flash frozen, lysed, and analyzed by Western blot. We found that TLR4-mediated anti-inflammatory signaling pathways were induced in h*RETN*Tg$^+$ mice (Fig. 3*E*). In particular, phosphorylation of TBK1 was increased and NF-κB inhibitor, alpha (IκBα) protein degradation was decreased. Given that the TRIF/TBK1/IRF signaling pathway mediates LPS-induced IL-10 production (25), and IκBα inhibits NF-κB activity (26), this differential TLR4 signaling suggests hRetn selectively induces an anti-inflammatory response. In addition, there were elevated levels of phosphorylated STAT3, suggesting increased IL-10 signaling (27). Together, these data suggest *Nb*-induced hRetn expression protects from endotoxic shock by promoting anti-inflammatory signaling pathways.

Human Resistin Binds to TLR4. To identify the downstream mechanism by which hRetn inhibits LPS-induced inflammation, we investigated the contribution of putative hRetn receptors. There are currently two proposed receptors for hRetn: TLR4 (19) and cyclic adenylate associated protein 1 (CAP1) (20). Both studies used human cell lines to demonstrate that hRetn promotes TNFα or IL-6 production through TLR4 or CAP1. However, it is unclear how hRetn interacts with these receptors in vivo. We investigated RNA-seq datasets from naive or *Nb*-infected lungs of h*RETN*Tg$^-$ and h*RETN*Tg$^+$ mice for differential expression of *Cap1* and *Tlr4* (13). Although *Cap1* expression was not influenced by *Nb* infection, *Tlr4* expression was significantly induced by *Nb* infection (Fig. 4*A*). Helminth infections can introduce endosymbiotic bacteria or create tissue injury leading to increased TLR4 expression to combat potential bacterial infections (28). Furthermore, only *Tlr4* expression was increased in h*RETN*Tg$^+$ mice (Fig. 4*A*), suggesting hRetn may promote expression of its own receptor. We next used the hRetn cellular binding assay to test whether hRetn binding was through TLR4. Dissociated lung cells from *Nb*-infected *Tlr4*$^{+/+}$ or *Tlr4*$^{-/-}$ mice were incubated with hRetn, followed by capture with detection antibodies to hRetn, as previously described (13). Although *Tlr4*$^{+/+}$ monocytes (Ly6C$^+$CD11b$^+$) were able to bind hRetn, hRetn binding was significantly abrogated in *Tlr4*$^{-/-}$ monocytes (Fig. 4*B*). We quantified TLR4-dependent binding as percentage hRetn-bound cells and mean fluorescence intensity in monocytes, alveolar macrophages (F4/80$^+$CD11c$^+$), and neutrophils (Ly6G$^+$CD11b$^+$) (Fig. 4 *C* and *D*). We observed TLR4-dependent binding in monocytes and alveolar macrophages, but not neutrophils, where hRetn binding in the absence of TLR4 was not noticeably affected. Although TLR4 is a receptor for hRetn, there are alternate hRetn receptors, which may be selectively expressed by different cell types. Thus, neutrophils could preferentially express an unidentified receptor for hRetn, which binds to and modulates the proinflammatory response through an alternative pathway. We evaluated the relative contribution of each hRetn-bound immune cell population by measuring their frequency in the lung (Fig. 4*E*). By this measurement, monocytes were the dominant cell type that bound resistin, followed by neutrophils and alveolar macrophages (Fig. 4*F*). Although the frequency of hRetn-bound cells was relatively low (15% in monocytes and 8% in neutrophils), this low frequency of hRetn responsive cells was nevertheless sufficient to prevent fatal endotoxic shock. We stained for B cells, T cells, and eosinophils; however, we did not observe any other significant population that bound hRetn.

Given that there are no publicly available CAP1-deficient mice, we examined direct protein–protein interaction of hRetn to TLR4 or CAP1 as an alternative to cell binding assays. A pull-down assay was performed using recombinant hRetn with histidine (his)-tagged human TLR4, his-human CAP1, or his-maltose binding protein (MBP) as a negative control (Fig. 4*G*). In the pull-down elution, Western blot using anti-his antibody confirmed that his-MBP, his-TLR4 and his-CAP1 are all pulled down by the nickel-NTA agarose beads. In addition, when blotting the elution fraction with anti-hRetn antibody, hRetn was only present in the elution with his-TLR4, not his-CAP1 or his-MBP. To ensure that this interaction was not a result of low-level LPS contamination, we also performed this pull-down assay with mammalian cell-derived hRetn. Similar to *E. coli*-derived hRetn, mammalian-derived hRetn is only detected when pulled down with his-TLR4, not his-CAP1 or his-MBP. Unlike the previous studies, where immunoprecipitation was performed with cell lysates, these data provide direct evidence that hRetn binds to TLR4 and does not require other proteins to form a complex. Although hRetn does not directly bind to CAP1, these data do not exclude the possibility that hRetn might bind to CAP1 if other adaptor proteins are present.

hRetn Competes with LPS/MD2 for Binding to TLR4. Although the X-ray crystal structure of hRetn is not available, we used the crystal structure of mouse Retn and human TLR4 to model hRetn binding to TLR4. This revealed that hRetn (green) and mRetn (cyan) have the same basic structure: a trimer consisting of a triple-helix stem (N-terminal domain) and a jelly-roll-like head (C-terminal domain) (Fig. 5*A*). Next, we used the ClusPro program to predict the interactions between hRetn and TLR4 (29). First we docked MD2, the adaptor protein that mediates LPS binding to TLR4, and found that several possible solutions proposed by ClusPro closely match the solved crystal structure of the complex (30) (Fig. 5*B*). Subsequently, we docked the model of hRetn into human TLR4 and found that several solutions place the N-terminal of hRetn hexamer (blue) within the binding pocket of TLR4 (red) for MD2 (white). In various predicted docked models obtained with ClusPro, the junction between the stem and head fits into the inner face of the horseshoe-like TLR4 molecule, obstructing the binding domain for MD2 and LPS (30). In these poses, several Retn side chains interact with different regions of the TLR4 to make ionic interactions and hydrogen bonds (Fig. 5*C*). On the basis of these structural predictions, we hypothesized that hRetn may sterically block LPS/MD-2 from binding to TLR4, thereby inhibiting LPS-induced inflammation. To investigate this possibility, in vitro competitive resistin/LPS binding assays were performed on human PBMCs. Evaluation of hRetn binding in human PBMC revealed that CD11b$^+$CD14$^+$ monocytes were the dominant population that bound hRetn, followed by SSC^{hi}CD11b$^+$CD16$^+$ neutrophils (Fig. 5*D*). We therefore assessed the potential for hRetn to block LPS binding in monocytes. Monocytes were able to bind LPS; however, binding was significantly abrogated if cells were preincubated with hRetn (Fig. 5 *E* and *F*). To determine whether hRetn inhibited downstream LPS function, we examined human PBMCs that had been preincubated with PBS or hRetn followed by LPS stimulation. PBMCs treated with only LPS

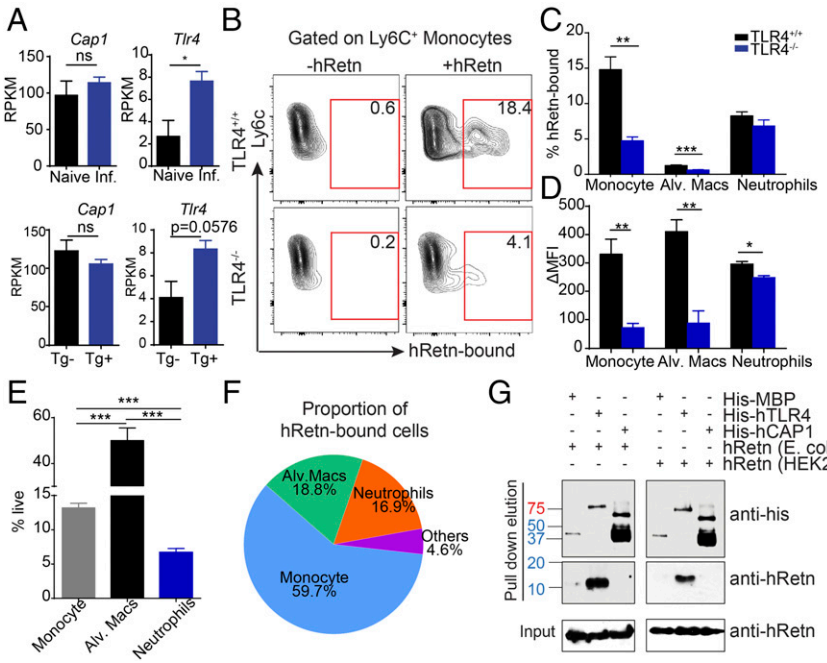

Fig. 4. TLR4 is a receptor for hRetn. (*A*) *Cap1* and *Tlr4* mRNA expression in naive or day 7 *Nb*-infected lungs from h*RETN*Tg^{-} and h*RETN*Tg^{+} lungs, as measured by RNA-seq. (*B–D*) hRetn binding of day 7 *Nb*-infected *Tlr4*$^{+/+}$ and *Tlr4*$^{-/-}$ lung cells was measured as frequency of hRetn-bound cells and Δmean fluorescence intensity. (*E*) Lung population frequency. (*F*) Pie chart of proportion of hRetn-bound cells. (*G*) Anti-His or anti-hRetn Western blot of pull-down assay with His-tagged TLR4, His-CAP1 or His-MBP with *E.coli* or 293T cell-derived hRetn. Mouse data are presented as mean ± SEM (n = 3–4 per group), and all data are representative of two to three separate experiments. ns, not significant; *$P \leq 0.05$; **$P \leq 0.01$; ***$P \leq 0.001$.

generated significantly more TNFα than cells treated with hRetn+LPS, demonstrating a functional inhibition of LPS-induced inflammation (Fig. 5*G*). These results were not an effect of endotoxin contamination, as the recombinant hRetn used in these studies was derived from HEK293 cells. In addition, as LPS can activate both TLR4 and TLR2, we used ultrapure LPS derived from *Salmonella minnesota*, which only binds to and activates TLR4.

We next evaluated the accuracy of the hRetn/TLR4 modeling, which predicted binding of the hRetn N-terminal helix to hTLR4. To this end, we used a solid phase synthesizer to generate an hRetn *N*-peptide (1–23 a.a.) and test its helical structure and function. The N-terminal sequence of hRetn contains many amino acids known to have a high propensity to form and stabilize alpha helices (31). For example, the presence of an RxxE motif, which may allow the two amino acids side chains to form an intramolecular salt bridge and would help stabilize the alpha helix in both the full-length form and the synthesized peptide. Circular dichroism analysis revealed that the synthetic agent has a significant alpha-helical content in solution, with negative bands around 208 and 222 nm and a positive band at 190 mm (Fig. 5*H*). Given the small size of the hRetn *N*-peptide and lack of specific antibodies to the *N*-peptide, it was not possible to perform the hTLR4 pulldown assay with the *N*-peptide. Instead, we tested the

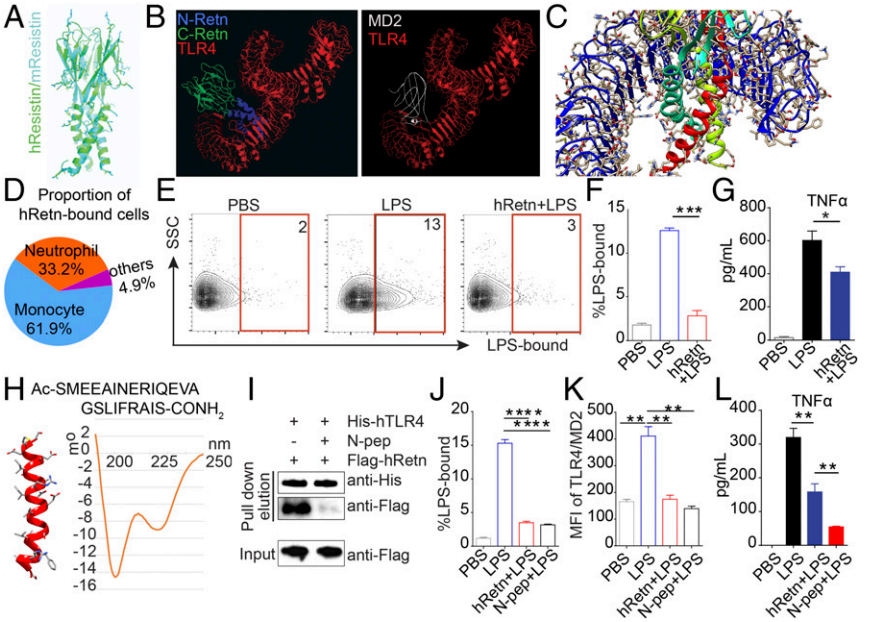

Fig. 5. hRetn outcompetes LPS for binding to TLR4. (*A*) Prediction of the hRetn (green) structure based on the structure of mRetn (cyan) was performed with ClusPro web server. (*B*) Structural modeling of hRetn (blue, N-terminal; green, C-terminal) and TLR4 (red) reveals that hRetn binds in the same binding pocket of MD2 (white), the adaptor protein for LPS. (*C*) Predicted molecular interactions between the N-terminal helical trimer (cyan, red, yellow) and the TLR4 monomer (blue). (*D*) Pie chart of proportion of hRetn-bound cells in human PBMC. (*E* and *F*) LPS binding assay in human PBMC with or without prior incubation with hRetn (*Left*), followed by flow cytometric analysis of LPS-bound CD14^{+}CD11b^{+} monocytes (*E*) and statistical analysis (*Right*) (*F*). (*G*) TNFα secretion measured in PBMC treated with PBS or hRetn followed LPS stimulation. (*H*) Primary sequence of the synthesized hRetn N-terminal peptide and CD spectrum of the agent measured at 100 μM. (*I*) His-tagged TLR4 was incubated with control buffer or hRetn N-terminal peptide (*N*-pep), followed by incubation with 293T cell-derived Flag-tagged hRetn, His-pulldown, and Western blot with anti-His and anti-Flag. (*J* and *K*) LPS binding assay in human PBMC with or without prior incubation with hRetn or *N*-pep followed by flow cytometric analysis of monocytes for LPS binding (*J*) and MD2/TLR4 surface expression (*K*). (*L*) TNFα secretion was measured in PBMC treated with PBS, hRetn, or *N*-pep, followed by LPS stimulation. PBMC data are presented as mean ± SEM (n = 3–4 replicates), and all are representative of two to three separate experiments. *$P \leq 0.05$; **$P \leq 0.01$; ***$P \leq 0.001$.

ability of the hRetn *N*-peptide to competitively inhibit subsequent hRetn binding, using the anti-Flag antibody to detect Flag-tagged full-length hRetn. Preincubation of hTLR4 with the hRetn *N*-peptide was sufficient to abrogate binding of full-length hRetn binding (Fig. 5*I*).

Last, we tested the functional ability of the hRetn *N*-peptide to block LPS binding and function. We performed the binding experiments on ice to rule out the effects of LPS-induced TLR4 endocytosis, which would have added complexity for interpretation of the data. Preincubation of human PBMC with the hRetn *N*-peptide or full-length hRetn inhibited LPS binding to $CD14^+CD11b^+$ monocytes (Fig. 5*J*). We tested whether the mechanism of inhibition was by preventing MD2/TLR4 complex formation. Flow cytometric analysis of surface MD2/TLR4 revealed that LPS treatment promoted MD2/TLR4 complex formation, but this was abrogated by hRetn or hRetn *N*-peptide (Fig. 5*K*). Functionally, the hRetn *N*-peptide was significantly more efficient at suppressing LPS-induced TNFα than full-length hRetn (Fig. 5*L*). These data suggest hRetn binds TLR4 through its N-terminal helix and effectively inhibits LPS binding and proinflammatory function. Together, these studies support the findings from our h*RETN*Tg^+ mouse model and validate that hRetn also inhibits LPS responsiveness in human immune cells.

hRetn Regulates Anti-Inflammatory Signaling Pathways Through TLR4. To investigate whether hRetn signals through TLR4, we generated h*RETN*Tg^+*Tlr4*$^{-/-}$ mice on a m*Retn*$^{-/-}$ background. Because *Tlr4*$^{-/-}$ mice are resistant to endotoxic shock, we investigated whether hRetn had TLR4-dependent anti-inflammatory effects under homeostatic conditions. Western blot for anti-inflammatory signaling molecules was performed on unstimulated peritoneal cells recovered directly from h*RETN*Tg^- or h*RETN*Tg^+ mice on the *Tlr4*$^{+/+}$ or *Tlr4*$^{-/-}$ background. Consistent with an anti-inflammatory function for hRetn, peritoneal cells from h*RETN*Tg^+*Tlr4*$^{+/+}$ mice had increased pSTAT3 and pTBK-1 and decreased IκBα degradation compared with h*RETN*Tg^-*Tlr4*$^{+/+}$ mice (Fig. 6*A*). However, this anti-inflammatory effect was abrogated in the absence of TLR4, where there was no significant difference between h*RETN*Tg^+*Tlr4*$^{-/-}$ and h*RETN*Tg^-*Tlr4*$^{-/-}$ mice. Peritoneal cells from naive mice were also characterized by flow cytometry, which revealed modest increases in monocytes and neutrophils in h*RETN*Tg^+ compared with h*RETN*Tg^- mice on the *Tlr4*$^{-/-}$ background but no significant differences in other cell populations, and on the *Tlr4*$^{+/+}$ background (Fig. 6*B*).

To determine whether hRetn effects on TLR4 signaling were dependent on the TBK1 and STAT3, human PBMC functional assays with TBK1 and STAT3 pharmacologic inhibitors were conducted. hRetn pretreatment with control DMSO significantly reduced LPS-induced TNFα secretion and conversely increased IL-10 expression (Fig. 6*C*). However, treatment with a TBK1 inhibitor before PBS or hRetn addition resulted in significantly reduced LPS-induced TNFα and conversely increased IL-10 expression. This suggests that LPS-induced TBK1 signaling is inflammatory in human PBMC and is consistent with the dual proinflammatory and anti-inflammatory functions for TBK1 dependent on the context (32, 33). Given that TBK1 inhibitor treatment itself caused a similar anti-inflammatory effect to hRetn, it is difficult to definitively conclude whether hRetn functions through TBK1. Nonetheless, hRetn's functional effect was abrogated in the presence of TBK1 inhibitor, suggesting that hRetn cannot further down-regulate TNFα or up-regulate IL-10 in the absence of TBK1 signaling. hRetn's functional effect was also abrogated when STAT3 signaling was inhibited. Combined, these in vivo and in vitro data suggest that under homeostatic conditions, hRetn binds to TLR4 and promotes STAT3 and TBK1 signaling to prevent LPS proinflammatory effects.

Discussion

Despite major breakthroughs in the understanding of sepsis progression, sepsis still has a high mortality rate of 30% (1). This is the result of a lack of effective treatment options, and many recent clinical trials have failed to reduce mortality in septic patients (4). Thus, alternative treatments for sepsis are urgently needed. One main pathogenic feature of sepsis is excessive inflammatory cytokine production, known as the systemic inflammatory response syndrome, which contributes to septic shock and mortality. Here, we identify a mechanism for hRetn in protecting against endotoxic shock by blocking LPS–TLR4 interaction and excessive production of proinflammatory cytokines. We employ two hRetn-expressing transgenic mouse lines, exogenous recombinant hRetn treatment, and human PBMCs cultures, to show that hRetn is critically protective against fatal LPS-induced endotoxic shock.

Clinical studies show that patients suffering from sepsis have elevated hRetn expression; therefore, it was initially believed that hRetn contributes to sepsis by promoting inflammation (15). This assumption was based on reports that LPS induces hRetn expression, and that hRetn increases proinflammatory cytokines production in vitro (16, 17). Our data confirm that hRetn expression is increased during septic shock. However, rather than promoting inflammatory cytokines and LPS-induced mortality, we propose that hRetn acts as a feedback mechanism to control systemic inflammation by binding and inhibiting TLR4 signaling. Although patients with more severe clinical scores for sepsis have more circulating hRetn, our data suggest that the increased hRetn expression may be the body's attempt to limit the excessive inflammatory immune response. Given these preclinical sepsis data, more specific studies investigating sepsis outcome and hRetn function are warranted to test the anti-inflammatory and therapeutic function of hRetn in sepsis pathogenesis.

There are currently two proposed receptors for hRetn: TLR4 and CAP1 (19, 20). Although our data show a direct interaction between TLR4 and hRetn, we used h*RETN*Tg^+*Tlr4*$^{-/-}$ mice to demonstrate that there are alternate receptors for hRetn. Interestingly, TLR4 deficiency abrogated the anti-inflammatory effect of hRetn in naive mice, suggesting that hRetn's immunoregulatory effect is dependent on its functional interaction with TLR4. The potential role of CAP1 in hRetn-mediated inhibition of LPS function is unclear. Our data suggest that CAP1 is unlikely to directly mediate protection during endotoxic shock. First, we were unable to detect hRetn in the pull-down fraction with his-tagged CAP1, suggesting there is no direct interaction between hRetn and CAP1. Second, CAP1 is an intracellular receptor, with no predicted transmembrane domain (20); thus, endocytosis of hRetn mediated by TLR4 would be necessary for interaction with CAP1. Previous studies have identified TLR4 as a putative receptor for hRetn; however, we prove direct hRetn-TLR4 interaction that functionally affects LPS-induced signaling and function. In addition, we provide functional evidence that hRetn inhibits LPS binding to human immune cells and subsequent LPS inflammatory function through a STAT3- and TBK1-dependent mechanism. Through structural modeling and experimental studies with the N-terminal peptide of hRetn, we conclude that hRetn interacts with the TLR4 monomer and inhibits binding of the MD2 adaptor protein. Competitive coimmunoprecipitation and human PBMC functional assays showed that the hRetn N-terminal is sufficient to bind to TLR4 and inhibit LPS-induced proinflammatory effects. These results support the hRetn N-terminal as the active domain of hRetn and offer the therapeutic possibility of using stand-alone hRetn N-terminal helices to inhibit LPS function.

There is 60% sequence homology between mRetn and hRetn; however, mRetn expression is restricted to adipocytes, whereas hRetn is predominantly expressed in myeloid cells (34). Given

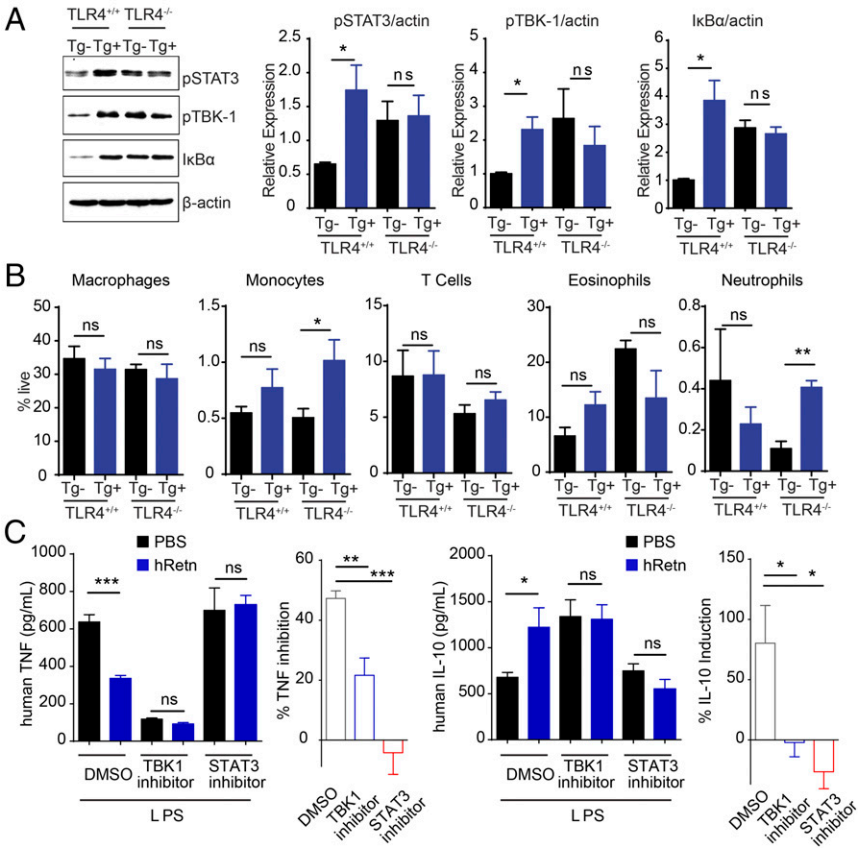

Fig. 6. hRetn downstream signaling is TLR4-dependent. PECs were collected from 6- to 8-wk-old naive h*RETN*Tg^{+} or h*RETN*Tg^{-} mice on the *Tlr4*$^{+/+}$ or *Tlr4*$^{-/-}$ background and analyzed directly ex vivo. (*A*) Representative Western blot (*Left*) and band density of phosphorylated STAT3, phosphorylated TBK1, and IκBα over endogenous β-actin was quantified for three to four mice per group (*Right*). (*B*) Flow cytometric analysis of PEC populations. (*C*) The ability of hRetn to inhibit LPS-induced TNFα and IL-10 secretion was measured in human PBMC pretreated with control DMSO, TBK1, and STAT3 inhibitors, followed by hRetn and LPS treatment. Percentage TNFα inhibition or IL-10 induction by hRetn over PBS-treatment was calculated. Data are presented as mean ± SEM (n = 3–4) and representative of two separate experiments. ns, not significant; *$P \leq 0.05$; **$P \leq 0.01$; ***$P \leq 0.001$.

this caveat, we used transgenic *hRETN*Tg^{+} mice on a m*Retn*$^{-/-}$ background, where we validated hRetn expression by macrophages and monocytes (13, 16). Both C57BL/6 (m*Retn*$^{+/+}$) mice and m*Retn*$^{-/-}$ mice were equally susceptible to LPS-induced mortality, suggesting that endogenous m*Retn* does not inhibit LPS function. The differential expression pattern of mRetn and hRetn, may explain this dichotomy in function, whereby mRetn affects metabolic function and hRetn is expressed systemically where it has an immunoregulatory function.

Although neutrophils act to limit initial bacterial or viral infection, they can also contribute to sepsis through excessive production of proinflammatory cytokines. In addition, neutrophils contribute to organ failure and hypoperfusion through the production of proteolytic enzymes, reactive oxygen species, and neutrophil extracellular traps (18, 21). We observed that hRetn inhibited neutrophil responses associated with a decrease in the neutrophil chemoattractant GM-CSF (35), but hRetn's effect on neutrophils may depend on the inflammatory context. In an LPS-alone model, hRetn reduced total neutrophil recruitment. In contrast, hRetn increased neutrophil numbers in *Nb*+LPS-treated mice, but this increased neutrophilia was associated with protection from endotoxic shock. Recent studies have shown that helminth-induced neutrophils are significantly different from LPS-induced neutrophils and are not proinflammatory (24); therefore, it is likely that the hRetn-induced neutrophils in *Nb*-infected mice did not contribute to LPS-induced inflammation.

hRetn binding assays of mouse and human immune cells revealed that monocytes were the main cell-type that bound hRetn. In addition, monocyte frequencies were increased in vivo in h*RETN*Tg^{+} mice and recombinant hRetn-treated mice. Together, these data suggest that monocytes are the main downstream cellular target of hRetn, where hRetn acts to suppress inflammatory pathways while promoting anti-inflammatory signaling through binding TLR4. Although monocytes express TLR4, nonimmune cells such as epithelial cells and endothelial cells can induce TLR4 expression in inflammatory settings (36). In addition, hRetn has been reported to act on endothelial cell lines (37). Given that vascular dysfunction is a significant contributing factor to sepsis pathogenesis, the possibility that hRetn influences endothelial cell function warrants further investigation. Notwithstanding this, our data strongly support an immunoregulatory function for hRetn through direct effects on monocytes.

Homeostatic levels of hRetn in the transgenic mice were only 50% protective against fatal endotoxic shock. Instead, low-dose LPS treatment or *Nb* infection was required to boost circulating hRetn levels for optimal protection against subsequent endotoxic shock. It is possible that hRetn provides protection through a similar mechanism to endotoxin tolerance, whereby hRetn stimulation of TLR4 signaling causes desensitization of the LPS/TLR signaling pathway (25, 38). TLR4 can induce two signaling pathways: MyD88/NFκB, which is proinflammatory, and TRIF/TBK1, which is anti-inflammatory and promotes IL-10 expression (38). h*RETN*Tg^{+} mice exhibited a TLR-4-dependent increase in TBK-1 signaling, but a decrease in NF-κB signaling, supporting a model in which hRetn binds to TLR4 and preferentially activates TRIF/TBK1. Consistent with this, h*RETN*Tg^{+} mice exhibited increased IL-10 production and IL-10-associated signaling in the endotoxic shock model. IL-10 production during sepsis is protective because it suppresses the production of TNFα and IL-6 through activation of STAT3 signaling (39). These results suggest that hRetn binding to TLR4 may decrease inflammation in two ways: by inhibiting LPS binding and proinflammatory signaling while increasing TBK1 activity and IL-10 production. Future studies using STAT3- or TBK1-deficient or knockdown immune

cells are warranted to delineate the contribution of STAT3 or TBK1 in the anti-inflammatory function of hRetn.

Although helminth infection is associated with an increase in circulating LPS, there are numerous helminth-mediated immunoregulatory mechanisms in place to reduce LPS-associated inflammatory response. For example, helminths infections are beneficial in sepsis by inducing IL-10 expression (6), and *Fasciola hepatica* secretes fatty acid binding proteins to reduce inflammatory responses (8). Our data suggest hookworm infection also protects from sepsis through hRetn-dependent and hRetn-independent mechanisms. *Nb*-infected h*RETN*Tg$^-$ mice were more resistant to LPS-induced mortality compared with naive h*RETN*Tg$^-$ mice. However, hRetn significantly enhanced *Nb*-induced protection from endotoxic shock. These data map hRetn as a helminth-induced regulatory pathway upstream of IL-10 expression. The complexity of host–helminth interaction is the result of millions of years of coevolution. For optimal outcome, the infected host must effectively balance the immune response to limit damage caused not only by the pathogen but also by excessive inflammation. This balance is essential when the host is coinfected with a variety of pathogens, such as helminths and bacteria. In this study, we show that although hRetn exacerbates helminth burden, it protects the host from excessive inflammation caused by endotoxic shock by blocking interaction between LPS and TLR4. In turn, this mechanism is exploited by helminths to prevent their own expulsion.

Previous studies on hRetn have defined it as a detrimental protein not only in sepsis but also in obesity, atherosclerosis, and rheumatoid arthritis (10, 11, 34). Our study identifies a beneficial function for hRetn, which may have evolved as a protective mechanism against sepsis, and suggests that reexamination of the therapeutic function of hRetn in modulating TLR4 signaling is warranted. Because the options for treatment against sepsis are limited, investigating the hRetn-immunoregulatory pathway or testing hRetn N-terminal based reagents could provide a therapy to mitigate the proinflammatory milieu found during sepsis.

Materials and Methods

Mice. Human resistin transgenic mice were generated as previously described on a mouse *Retn*$^{-/-}$ background (16). Briefly, the human resistin gene, along with 21,300 bp upstream and 4,248 bp downstream of the human resistin start site, was inserted through a bacterial artificial chromosome. Genome insertion of h*RETN* in the two transgenic mouse lines was determined by Dartmouse, which sequences and analyzes thousands of SNPs throughout the mouse genome. For the endotoxic shock model, mice were injected i.p. with two doses of LPS (Sigma): 0.05 mg/kg LPS followed by 12 mg/kg LPS (females) or 20 mg/kg LPS (males) 12 h later. Mice were monitored at least twice a day and killed according to humane endpoints. For treatment with recombinant resistin, C57BL/6 mice were injected i.p. with PBS or 0.5 μg hRetn (Peprotech). *Nb* life cycle was maintained in Sprague-Dawley rats, as previously described (13). Mice were anesthetized with isoflurane and injected s.c. with 500 L3 larvae. Serum collection was by retro-orbital bleeding, and body temperature was measured by rectal thermometer (Braintree Scientific). All animals in the experiment were age-matched (6–8 wk old), sex-matched, and housed in a specific pathogen-free facility.

Vascular Permeability Assay. Evan's blue dye was used to measure vascular permeability. Mice were anesthetized by isoflurane, and 200 μL of 0.5% Evan's Blue dye in PBS was injected retro-orbitally. After 10 min, mice were killed by CO_2 and perfused with 20 mL PBS. Tissue was excised, weighed, and incubated with 500 μL N, *N*-dimethylformamide (Sigma) for 24 h at 55 °C. Extracted Evan's blue was measured at 610 nm according to a standard curve.

Binding Assay and Flow Cytometry. Single-cell suspension of lung tissue was prepared and hRetn binding was measured as previously described (13). Briefly, dissociated lung cells were incubated for 1 h at 4 °C with 0.5 μg recombinant hResistin (Peprotech) or PBS, followed by 2× wash in FACS buffer, incubation with Fc block (5 μg/mL αCD16/32 and 10 μg/mL purified rat IgG1, 5 min at 4 °C). Cells were stained with biotinylated α-hRetn (30 min at 4 °C; Peprotech) followed by detection with BV605-conjugated streptavidin (BD) and surface marker antibodies. The peritoneal cavity was washed and PECs recovered in 5 mL ice cold PBS. Surface marker antibodies were F4/80 (clone A3-1), SiglecF (clone E50-2440), CD4 (clone RM4-5), Ly6C (HK1.4), CD11b (clone M1/70), CD11c (clone N418), Ly6G (clone 1A8), MHCII (clone M5/114.15.2), CD3e (clone 145–2C11), and CD115 (clone AFS98), purchased from Affymetrix, BD Biosciences, or Biolegend. Cell populations were determined as follows: peritoneal macrophage (F4/80$^+$CD11b$^+$), neutrophils (Ly6G$^+$CD11b$^+$), eosinophils (SiglecF$^+$CD11c$^-$), monocyte (Ly6C$^+$CD11b$^+$), alveolar macrophages (F4/80$^+$CD11c$^+$). For flow cytometric analysis, all samples were run on a BD LSRII and analyzed on FlowJo (v10).

Human PBMC. Human buffy coat was purchased from Zen-bio. Buffy coat was overlaid on top of Histopaque-1077 and spun at 700 × *g* at 25 °C with no brake, and PBMCs were recovered from the interphase. PBMCs were plated in 96-well plates and stimulated with mammalian-derived human resistin (1 μg/mL; LifeSpan Biosciences) or hRetn *N*-peptide (1 μg/mL). After 24 h, ultrapure LPS (100 ng/mL; InvivoGen) was added and supernatants recovered for ELISA at 24 h. Where indicated, cells were incubated for 4 h with STAT3 (5, 15-DPP, 50 μM) or TBK1 (BX-795, 1 μM) inhibitors before hRetn treatment. For the hRetn competitive binding assay, 1×10^6 cells were incubated with recombinant hRetn (0.5 μg), washed in PBS, and then incubated with 0.5 μg LPS-biotin (incubations were 30 min on ice). Cells were washed in FACS buffer, treated with Fc block, and stained with BV605-conjugated streptavidin and α-human primary antibodies: CD14 (clone M5E2), CD11b (clone M1/70), and MD2/TLR4 (clone MTS510), purchased from Affymetrix.

Cytokine Quantification. Sandwich ELISAs were performed using capture and biotinylated antibodies for human resistin (Peprotech), IL-10, and TNFα (BD Biosciences) according to manufacturer's instructions. Detection was performed with streptavidin-peroxidase (Jackson ImmunoResearch) and TMB peroxidase substrate (BD Biosciences), followed by addition of 2N H_2SO_4. Optical density was captured at 450 nm. Samples were compared with serial-fold dilution of recombinant protein. For Luminex, inflammatory cytokine kits (Affymetrix) were run according to manufacturer's instructions and quantified on Luminex MagPix (Luminex Corp.). For cytokine bead array, cytokine kits from BD Bioscience were run according to manufacturer's instructions on BD LSRII and analyzed using FCAP Array Software.

LAL Assay. Recombinant hResistin was tested for endotoxin contamination using the Pierce *Limulus* Amebocyte Lysate assay (Thermo Scientific) according to manufacturer's instructions under sterile conditions.

Pull-Down Assay. First, 1 μg/mL protein His-tagged MBP, human TLR4, and human CAP1 were added to nickel-nitrilotriacetic acid-agarose beads (Invitrogen) in binding buffer (50 mM NaH_2P0_4, 500 mM NaCl, 10 mM Imidazole at pH 8.0) and mixed for 1 h at 4 °C, followed by washing and 1 h incubation at 4 °C with hRetn (*E. coli*-derived, Peprotech, or 293T cell-derived; LifeSpan Biosciences) in binding buffer. Beads were washed in wash buffer (50 mM NaH_2P0_4, 500 mM NaCl, 20 mM Imidazole at pH 8.0), and complex protein eluted with elution buffer (50 mM NaH_2P0_4, 500 mM NaCl, 250 mM Imidazole at pH 6.0). His-MBP, His-TLR4, and His-CAP1 were detected by anti-His antibody (Abcam), and hRetn was detected by anti-hRetn antibody (donated by Mitchell Lazar) by Western Blot. For the *N*-peptide binding experiment, 1 μg/mL His-tagged human TLR4 with 500 ng/mL *N*-peptide or 10%TFE control was added to the beads in binding buffer and mixed for 30 min at 4 °C, followed by coimmunoprecipitation using 1 μg/mL Flag-hRetn (LifeSpan Biosciences), anti-His, or anti-Flag (Sigma).

hRetn N-Terminal Peptide Synthesis. hRetn N-terminal peptide (1–23 a.a.) was synthesized using a microwave- assisted solid-phase synthesizer (Liberty Blue; CEM Corp.) and a double coupling protocol. The agent was subsequently purified by reverse phase HPLC and characterized by high-resolution mass spectrometry and NMR. The soluble hRetn *N*-peptide helical content was determined by circular dichroism measurements in aqueous buffer containing 10% trifluoroethanol.

Signaling Western Blot. First, 1×10^6 peritoneal cells from one mouse or 3×10^6 cell pooled from three mice per group were lysed in RIPA buffer (150 mM sodium chloride, 1%Triton X-100, 1% sodium deoxycholate, 0.1% SDS, 50 mM Tris·HCl, 2 mM EDTA). Proteins were boiled in loading buffer (Bioland Scientific LLC), denatured, separated with SDS/PAGE gels, transferred to PVDF membranes (Millipore), and blocked with 5% BSA (Sigma) or 5% milk. Signaling proteins were detected with antibodies anti-pSTAT3 (Tyr705; Abcam), anti-pTBK1 (Ser172, clone D52C2), anti-IκBα, and anti-β-actin and then incubated with anti-rabbit or mouse HRP-conjugated IgG. All antibodies were purchased from Cell Signaling Technology. Proteins were detected with ECL (Pierce Chemical Co.) and exposed with X-ray film or ChemiDoc XRS+System (Bio-Rad). For quantification of protein levels,

appropriate film exposures were scanned and the density of bands was determined with Image J and normalized with endogenous β-actin.

Structural Predictions. The structural analysis of the TLR4–resistin interactions was performed with the structure of human TLR4–MD2–LPS complex (PDB code: 3FXI) and human resistin built by homology modeling. The sequence of human resistin was downloaded from the universal protein sequence (entry no. Q9HD89; Uniprot). Then, this sequence was used in SWISS-Model Server for homology modeling to find a structural template. This server found murine resistin (PDB code: 1RFX) as the template with maximum sequence identity of 57.61%. Murine resistin 3D structure was used to build the structural model for human resistin, using the server. The model of the trimer of human resistin was used perform docking studies, with the human TLR4 using the ClusPro web server to predict potential interactions of the resistin trimer to the TLR4 dimer based on Van der Waal's electrostatic interactions. As a control, models of the complex between MD2 and TLR4 were similarly generated and compared with the experimental X-ray structure of the complex, revealing an excellent agreement. PDBePISA server was used to confirm the feasibility of all of the models and detailed protein–protein interactions. Pymol software was used for all modeling manipulation.

Statistical Analysis. All statistics were generated on GraphPad Prism using, where appropriate, log rank test, Student *t* test, one-way ANOVA, or two-way ANOVA. ns, not significant (*$P \leq 0.05$; **$P \leq 0.01$; ***$P \leq 0.001$; ****$P \leq 0.0001$).

Ethics Statement. All protocols for animal use and euthanasia were approved by the University of California, Riverside, Institutional Animal Care and Use Committee (https://or.ucr.edu/ori/committees/iacuc.aspx; protocol A-20150028E) and were in accordance with the National Institutes of Health Guidelines. Animal studies are in accordance with the provisions established by the Animal Welfare Act and the Public Health Services Policy on the Humane Care and Use of Laboratory Animals. Human buffy coat (~60 mL concentrated leukocytes and erythrocytes) were collected from healthy donors with signed informed consent by Zen-bio, Inc. Isolation of PBMC and assays were performed with the approval of the University of California, Riverside (UCR), Institutional Review Board (HS-14–155, Exempt 4 category).

ACKNOWLEDGMENTS. We thank Ilhem Messaoudi and Norma Mendoza for assistance with the Luminex assays. These studies were supported by NIH (1R01AI091759-01A1 to M.G.N.; P01DK49210 to M.A.L.); UCR School of Medicine initial complement, UCR Academic Senate, UCR Office of Technology and Commercialization (to M.G.N.); and the American Association of Immunology (Careers in Immunology Fellowship to J.C.J. and M.G.N.). M.P. holds the Daniel Hays Chair in Cancer Research at the School of Medicine at UCR.

1. Angus DC, et al. (2001) Epidemiology of severe sepsis in the United States: Analysis of incidence, outcome, and associated costs of care. *Crit Care Med* 29:1303–1310.
2. Cauwels A, Brouckaert P (2007) Survival of TNF toxicity: Dependence on caspases and NO. *Arch Biochem Biophys* 462:132–139.
3. Roger T, et al. (2009) Protection from lethal gram-negative bacterial sepsis by targeting Toll-like receptor 4. *Proc Natl Acad Sci USA* 106:2348–2352.
4. Marshall JC (2014) Why have clinical trials in sepsis failed? *Trends Mol Med* 20: 195–203.
5. Szkudlapski D, et al. (2014) The emering role of helminths in treatment of the inflammatory bowel disorders. *J Physiol Pharmacol* 65:741–751.
6. Gondorf F, et al. (2015) Chronic filarial infection provides protection against bacterial sepsis by functionally reprogramming macrophages. *PLoS Pathog* 11:e1004616.
7. Goodridge HS, et al. (2005) Immunomodulation via novel use of TLR4 by the filarial nematode phosphorylcholine-containing secreted product, ES-62. *J Immunol* 174: 284–293.
8. Martin I, Cabán-Hernández K, Figueroa-Santiago O, Espino AM (2015) Fasciola hepatica fatty acid binding protein inhibits TLR4 activation and suppresses the inflammatory cytokines induced by lipopolysaccharide in vitro and in vivo. *J Immunol* 194:3924–3936.
9. Steppan CM, et al. (2001) The hormone resistin links obesity to diabetes. *Nature* 409: 307–312.
10. Reilly MP, et al. (2005) Resistin is an inflammatory marker of atherosclerosis in humans. *Circulation* 111:932–939.
11. Migita K, et al. (2006) The serum levels of resistin in rheumatoid arthritis patients. *Clin Exp Rheumatol* 24:698–701.
12. Montoya JG, et al. (2017) Cytokine signature associated with disease severity in chronic fatigue syndrome patients. *Proc Natl Acad Sci USA* 114:E7150–E7158.
13. Jang JC, et al. (2015) Macrophage-derived human resistin is induced in multiple helminth infections and promotes inflammatory monocytes and increased parasite burden. *PLoS Pathog* 11:e1004579.
14. Liu KT, et al. (2016) Serum neutrophil gelatinase-associated lipocalin and resistin are associated with dengue infection in adults. *BMC Infect Dis* 16:441.
15. Macdonald SP, et al. (2014) Sustained elevation of resistin, NGAL and IL-8 are associated with severe sepsis/septic shock in the emergency department. *PLoS One* 9: e110678.
16. Park HK, Qatanani M, Briggs ER, Ahima RS, Lazar MA (2011) Inflammatory induction of human resistin causes insulin resistance in endotoxemic mice. *Diabetes* 60: 775–783.
17. Lehrke M, et al. (2004) An inflammatory cascade leading to hyperresistinemia in humans. *PLoS Med* 1:e45.
18. Jiang S, et al. (2014) Human resistin promotes neutrophil proinflammatory activation and neutrophil extracellular trap formation and increases severity of acute lung injury. *J Immunol* 192:4795–4803.
19. Tarkowski A, Bjersing J, Shestakov A, Bokarewa MI (2010) Resistin competes with lipopolysaccharide for binding to toll-like receptor 4. *J Cell Mol Med* 14:1419–1431.
20. Lee S, et al. (2014) Adenylyl cyclase-associated protein 1 is a receptor for human resistin and mediates inflammatory actions of human monocytes. *Cell Metab* 19: 484–497.
21. Kovach MA, Standiford TJ (2012) The function of neutrophils in sepsis. *Curr Opin Infect Dis* 25:321–327.
22. Huang L, et al. (2014) Eosinophil-derived IL-10 supports chronic nematode infection. *J Immunol* 193:4178–4187.
23. Farid AS, Jimi F, Inagaki-Ohara K, Horii Y (2008) Increased intestinal endotoxin absorption during enteric nematode but not protozoal infections through a mast cell-mediated mechanism. *Shock* 29:709–716.
24. Chen F, et al. (2014) Neutrophils prime a long-lived effector macrophage phenotype that mediates accelerated helminth expulsion. *Nat Immunol* 15:938–946.
25. Chang EY, Guo B, Doyle SE, Cheng G (2007) Cutting edge: Involvement of the type I IFN production and signaling pathway in lipopolysaccharide-induced IL-10 production. *J Immunol* 178:6705–6709.
26. Scherer DC, Brockman JA, Chen Z, Maniatis T, Ballard DW (1995) Signal-induced degradation of I kappa B alpha requires site-specific ubiquitination. *Proc Natl Acad Sci USA* 92:11259–11263.
27. Weber-Nordt RM, et al. (1996) Stat3 recruitment by two distinct ligand-induced, tyrosine-phosphorylated docking sites in the interleukin-10 receptor intracellular domain. *J Biol Chem* 271:27954–27961.
28. George PJ, et al. (2012) Evidence of microbial translocation associated with perturbations in T cell and antigen-presenting cell homeostasis in hookworm infections. *PLoS Negl Trop Dis* 6:e1830.
29. Kozakov D, et al. (2017) The ClusPro web server for protein-protein docking. *Nat Protoc* 12:255–278.
30. Park BS, et al. (2009) The structural basis of lipopolysaccharide recognition by the TLR4-MD-2 complex. *Nature* 458:1191–1195.
31. Pace CN, Scholtz JM (1998) A helix propensity scale based on experimental studies of peptides and proteins. *Biophys J* 75:422–427.
32. Hemmi H, et al. (2004) The roles of two IkappaB kinase-related kinases in lipopolysaccharide and double stranded RNA signaling and viral infection. *J Exp Med* 199: 1641–1650.
33. Marchlik E, et al. (2010) Mice lacking Tbk1 activity exhibit immune cell infiltrates in multiple tissues and increased susceptibility to LPS-induced lethality. *J Leukoc Biol* 88: 1171–1180.
34. Schwartz DR, Lazar MA (2011) Human resistin: Found in translation from mouse to man. *Trends Endocrinol Metab* 22:259–265.
35. Khajah M, Millen B, Cara DC, Waterhouse C, McCafferty DM (2011) Granulocyte-macrophage colony-stimulating factor (GM-CSF): A chemoattractive agent for murine leukocytes in vivo. *J Leukoc Biol* 89:945–953.
36. Bäckhed F, Meijer L, Normark S, Richter-Dahlfors A (2002) TLR4-dependent recognition of lipopolysaccharide by epithelial cells requires sCD14. *Cell Microbiol* 4:493–501.
37. Pirvulescu MM, et al. (2014) Subendothelial resistin enhances monocyte transmigration in a co-culture of human endothelial and smooth muscle cells by mechanisms involving fractalkine, MCP-1 and activation of TLR4 and Gi/o proteins signaling. *Int J Biochem Cell Biol* 50:29–37.
38. Biswas SK, Lopez-Collazo E (2009) Endotoxin tolerance: New mechanisms, molecules and clinical significance. *Trends Immunol* 30:475–487.
39. Latifi SQ, O'Riordan MA, Levine AD (2002) Interleukin-10 controls the onset of irreversible septic shock. *Infect Immun* 70:4441–4446.